

Probing interstellar scattering towards the Galactic centre with pulsar VLBI*

Olaf Wucknitz[†]

Max-Planck-Institut für Radioastronomie, Auf dem Hügel 69, 53121 Bonn, Germany,

E-mail: wucknitz@mpifr-bonn.mpg.de

Temporal scatter-broadening can seriously affect our ability to find pulsars orbiting the central mass in our Galaxy. Many of these invaluable probes of geometry around the black hole are expected, but none have been found in close orbits so far, possibly as result of strong scattering. The magnetar PSR J1745–2900 discovered in 2013 at a separation of < 3 arcsec is not the optimal type of pulsar for studies of general relativity, but it can be used to investigate the scattering properties so that search strategies can be adapted accordingly.

This contribution presents an observation of this magnetar using short baselines between VLBI stations in Europe in a non-standard interferometry mode. The most important goal is determining the distance of the scattering screen, or the distribution of scattering material if not confined to one screen.

The analysis is based on phase-binned visibilities that allow measuring the shape of the scattering disk and how it grows with increasing delay over the scattering tail of the pulse profile. Narrow rings growing with the square root of delay are expected for a single thin scattering screen and the preliminary results are indeed consistent with this expectation. This means that most of the angular and temporal broadening is caused by the same and relatively thin scattering screen and that, in contrast to standard models of the interstellar scattering behaviour near the Galactic centre, this screen is located about halfway between the centre and us.

*12th European VLBI Network Symposium and Users Meeting,
7-10 October 2014
Cagliari, Italy*

*Original title of the conference talk: *Scattering as a nuisance and as a tool*

[†]Speaker.

1. Pulsars near black holes

The motivation for this project is the fact that pulsars closely orbiting a black hole can potentially be used to test general relativity and to determine parameters of the black hole with the highest precision. For these tests, we want to probe the geometry in strong gravitational fields (thus near a black hole). Our most accurate measurements are those of time, and in astronomy these also happen to be comparatively simple. It is thus a natural idea to use highly accurate clocks as probes of geometry and measure their ‘ticks’ for the analysis. Luckily nature is so kind to provide such accurate clocks in the form of pulsars.

One of the most promising candidate for a black hole within reasonable distance is the one in Sgr A* in the Galactic centre (GC) at a distance of about 8.5 kpc with a mass around 4 million Solar masses. The density of stars in that region is very high, and common formation scenarios predict an abundance of neutron stars and in particular pulsars in orbit around Sgr A*.

Liu et al. (2012) and others describe in detail, which parameters can be determined, e.g. the mass and spin of the GC black hole, allowing us to test the cosmic censorship conjecture, or the quadrupole moment so that the no-hair-theorem can be tested. Additionally perturbations from other masses can also be detected easily.

A potential major difficulty in finding these pulsars is the effect of interstellar scattering producing subimages that are deflected and thus delayed by different amounts. Such a range of delays can easily wash out the ‘pulsations’ that are used to identify pulsars, that form their clock ticks and are thus the basis of accurate timing measurements. Unfortunately the GC appears to be the region affected the worst, so that observing parameters have to be chosen that minimise the effects.

The deflection angles roughly scale with the observing wavelength as $\theta \propto \lambda^2$ and the delays with $\tau \propto \theta^2 \propto \lambda^4$, so that the effect becomes much stronger at low frequencies and that higher-frequency observations may be needed.¹ Exact numbers for the GC are highly model-dependent, but were thought to be as bad as hundreds of seconds for frequencies around 1 GHz, which would wash out the signals even from the slowest pulsars (Cordes & Lazio, 1997).

It has been tried to search for pulsars near the GC at high frequencies, e.g. with the GBT at 15 GHz (Macquart et al., 2010) and with Effelsberg at 19 GHz (Eatough et al., 2013b). Despite the expectations that at least dozens of pulsars should have been found, no single object could be detected in these surveys within 1–2 pc of the GC.

2. Interstellar scattering towards the Galactic centre

From the scattering geometry (Fig. 1) the relation between scattering angle θ (leading to the size of the scattering disk for the ensemble of all subimages) and the corresponding delay τ (leading to the temporal scattering tail) can be derived easily in the small-angle approximation:

$$c\tau = \frac{1}{2}\theta^2 D' \qquad D' = \frac{D(D-\Delta)}{\Delta}$$

Note how strongly the scattering delay for a given angular size θ depends on the distance Δ to the scattering screen. If it is very close to the pulsar (as expected for the GC), the delay becomes very

¹For Kolmogorov-type turbulence, the exponents are even slightly higher (2.2 and 4.4).

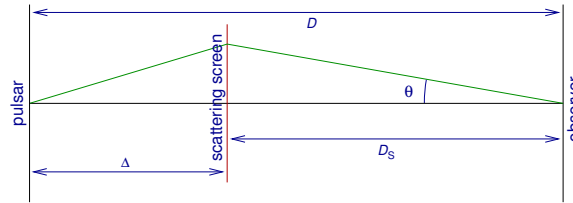


Figure 1: The fundamental scattering geometry with one subimage deflected by an angle θ , which causes a geometric delay of τ .

large, while it vanishes in the limit of a screen very close to the observer. The angular scattering size of Sgr A* is about 1 arcsec for a frequency of 1 GHz.

Taking the model value $\Delta = (133^{+200}_{-80})$ pc from Lazio & Cordes (1998), we would expect 150 sec at 1 GHz, while this scattering time reduces to 2 sec if the screen is halfway between the GC and us. Knowing the location of the scattering screen (or the distribution of scattering material) is thus of uttermost importance, not only to understand why we have not found any pulsars in that region until recently, but also to define our search strategy for the future.

3. The GC magnetar PSR J1745–2900

In April 2013, the Swift satellite detected an X-ray flare in the area of Sgr A* (Kennea et al., 2013). NuSTAR found pulsations with a period of 3.76 sec in the same object and identified it as a possible magnetar (Mori et al., 2013). Within days, the magnetar was also detected at radio frequencies (Eatough et al., 2013a) with the Effelsberg telescope and studied extensively since then (e.g. Shannon & Johnston, 2013).

Spitler et al. (2014) showed that the scattering time is proportional to $\lambda^{3.8}$, close to the expectation, and that at 1 GHz it is $\tau = 1.3$ sec, much less than derived from the models of Lazio & Cordes (1998). At the same time Bower et al. (2014) measured the size of the scattering disk with VLBI and found it to be consistent with that of Sgr A* itself. Combining these two results led to an estimated distance of the scattering screen from the magnetar of $\Delta = (5.9 \pm 0.3)$ kpc, provided that the temporal and angular scattering are caused by one and the same thin scattering screen.

4. Testing the one-screen hypothesis

Because of the conflict of the results of Spitler et al. (2014) and Bower et al. (2014) with standard GC models, the assumption of only one scattering screen has to be tested. In an alternative scenario there may be at least two scattering screens, one close to the GC, dominating the temporal scattering, and one closer to us, which then dominates the angular broadening. By comparing only the *mean* scattering angle (angular broadening) with the *mean* scattering delay (temporal broadening), the two scenarios cannot be distinguished. Our project aims at comparing θ with τ not on-average but for individual parts of the scattered signal, in the same way as described in more detail by Wucknitz (2013) for other targets. If both types of scattering are caused (or at least dominated) by the same scattering screen, we expect to see the scaling with $\tau \propto \theta^2$ if we can resolve the signal temporally and spatially at the same time. If, on the other hand, both effects are resulting from different screens, the temporal and angular effects would not be correlated.

5. Observations, correlation and calibration

The magnetar PSR J1745–2900 was observed by the LEAP² team on 9th Nov 2013 for about one hour with the Effelsberg 100 m dish, the Nançay radio telescope, the phased Westerbork array and the Lovell telescope, in the frequency range 1604–1732 MHz using baseband pulsar backends sampling with 8 bits/sample. The analysis presented here only uses the shortest baseline between Effelsberg and Westerbork, ranging (in projection) from 42 km at the beginning to 79 km towards the end of the scan. This is about the optimal range for the expected angular size.

Data were shipped to Bonn to be correlated using own software. In order to determine an unknown delay offset in the Effelsberg system, we cross-correlated the intensity variations from both stations and used the maximum at 409 msec as first estimate for the delay. The data were correlated in all four polarisation products after converting the Westerbork data to a circular basis. The delay was then refined by fringe-fitting the correlated visibilities. In this process and for the calibration, Sgr A* at a distance of 2''4 was used as in-beam calibrator. The calibrator and the target were separated with binned and weighted integrations of the correlations. For Sgr A*, only bins in the off-state of the pulsar are integrated, while for PSR J1745–2900 we integrate around the region of interest (pulse peak for the calibration) and subtract as much of the off-state to remove Sgr A* as good as possible.

We first calibrated on Sgr A*, taking into account delay, delay rate, varying parallactic angle and orientation of the receivers. We also tested the effects of dispersive delays and differential Faraday rotation due to the ionosphere, but it turned out that explicit corrections for these were not necessary. Bandpass correction was applied in amplitude and phase and the fringe-fitting and calibration procedure was re-iterated after this step. The position of the target relative to Sgr A* was then determined by a model-fit in uv -space, and the phase centre was shifted to that position.

6. Analysis and results

The calibrated visibilities for PSR J1745–2900 were then split into bins in pulse phase (for this preliminary analysis 0.1 sec in width) to represent the scattering delay (assuming an intrinsically narrow peak), and in time and thus baseline length to represent the angular structure.

As Fig. 2 shows, apparently the size of the scattering disk does indeed change with scattering delay, which proves that both effects are at least partly due to the same screen. The expectation is that, as function of delay, we see a circular ring that expands as $\theta \propto \sqrt{\tau}$. To test this, we fitted (again in uv -space) models of uniform (this will be refined in the future) circular rings with arbitrary radius and total flux to the data. Fig. 3 shows the model visibilities compared to the measurements.

Fig. 4 shows how the size of the scattering ring grows with time. Within the best range of the pulse peak, the size seems to follow the expected relation, which finally confirms that for this pulsar most of the temporal and angular scatter-broadening must be produced by *one* relatively thin screen. From the scaling constant we can estimate the effective distance $D' = 8.6$ kpc and from that the distance of the scattering screen from the pulsar, $\Delta = 4.2$ kpc, which localises the screen almost exactly halfway between the pulsar (assuming it is at the same distance as Sgr A*) and us.

²Large European Array for Pulsars, see Kramer & Champion (2013), Bassa et al. (in prep.) and <http://www.leap.eu.org/>.

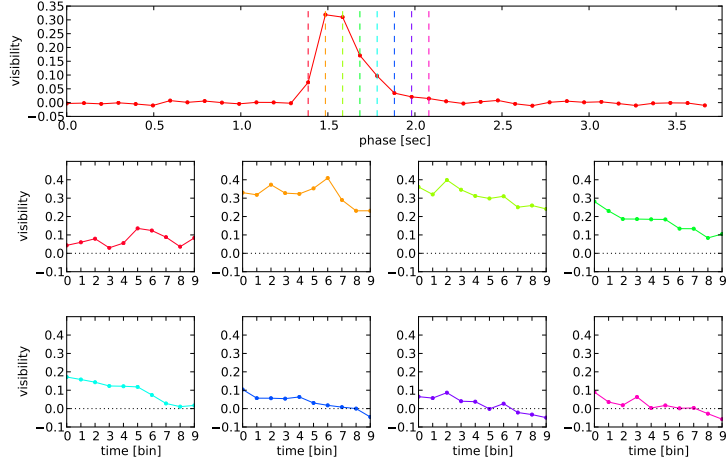


Figure 2: Visibility functions for different bins of the pulse peak (colour-coded and labelled on top). The horizontal axes on the lower plots show time within the scan, over which the baseline increases from 42 to 79 km. Near the peak these curves are relatively flat, corresponding to a compact source, but in the scattering tail they become steeper and even cross zero for large delays and the longest baselines.

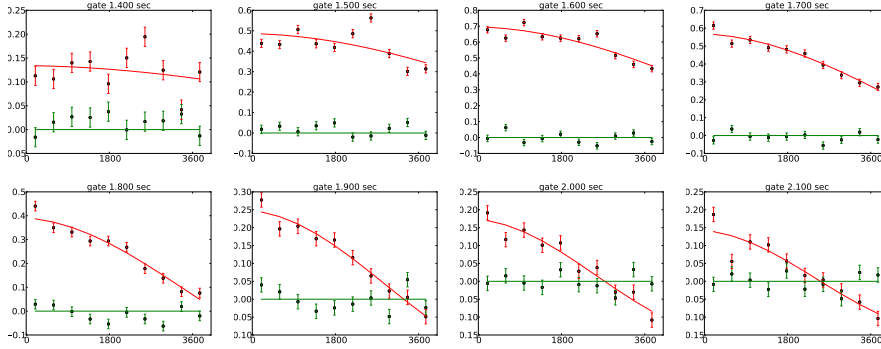


Figure 3: Visibility functions for the same bins as in Fig. 2 as function of time (in seconds). The real part is shown in red, the imaginary part in green. Error bars are measurements, curves are model fits of narrow rings. There are still systematic deviations resulting from flux variability, but the main structure is reproduced well.

We emphasise that this result is preliminary and that a number of refinements have to be included in the analysis (higher time-resolution, consider anisotropy, do consistent global fit, consider pulsar variability, include other baselines), before the final result can be derived and a realistic error estimate can be attempted. For the moment our result appears to be consistent with that of Spitler et al. (2014) and Bower et al. (2014), but we have now actually tested and proven the basic single thin screen assumption on which their analysis was based.

In view of this, we have to re-consider the models of the GC (e.g. Lazio & Cordes, 1998), taking into account the observational facts that went into those models, but also our new results and the arguments presented by van Langevelde et al. (1992). Finding the strongest scattering in a small region of the sky near Sgr A* is a strange coincidence, if the material causing it is not actually located directly around the GC, but apparently this conclusion cannot be avoided anymore.

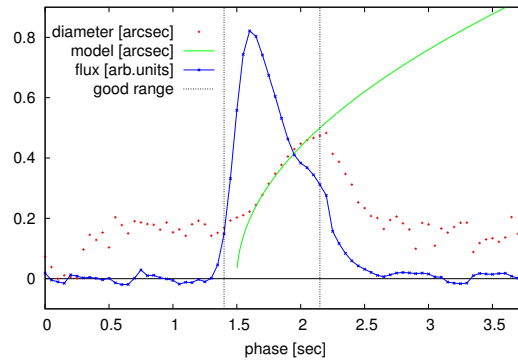


Figure 4: Results from fitting the diameter of the ‘scattering ring’ as function of pulse phase and thus scattering delay. The blue curve shows the total flux (pulse profile) and the red points are the diameters of the fitted rings in arcsec. Two vertical lines bracket the range with sufficient SNR. The green curve is a fit-by-eye of a $\theta \propto \sqrt{\tau}$ model to the most trustworthy data points. The deviating points near a phase of 1.5 sec are affected by the (in this preliminary analysis) low resolution in time and by the intrinsic pulse width.

Recent observations at higher frequencies (Spitler et al., in prep.) seem to indicate strong variations in the scattering delay with time. The most plausible explanation would be additional fast moving clouds near the GC. If they are sufficiently small, they would not affect the scattering size at our frequencies, and indeed they have to be small to explain the rapid variations. In the final analysis of our data (and of new observations in Nov 2014) we will have to take into account possible additional scattering material closer to the pulsar, in order to finally derive a picture that explains all the observational data consistently. This will form invaluable input for future pulsar searches near the black hole that is believed to be located in the centre of our Galaxy.

7. Acknowledgements

The author thanks the LEAP team for providing observing time and for help with the observations and the data transfer. Ralph Eatough is thanked for interesting discussions about the subject.

References

- Bower, G. C., Deller, A., Demorest, P., et al. 2014, *ApJ*, 780, L2
 Cordes, J. M. & Lazio, T. J. W. 1997, *ApJ*, 475, 557
 Eatough, R. P., Falcke, H., Karuppusamy, R., et al. 2013a, *Nature*, 501, 391
 Eatough, R. P., Kramer, M., Klein, B., et al. 2013b, in *IAU Symposium S291*, 382
 Kennea, J. A., Burrows, D. N., Kouveliotou, C., et al. 2013, *ApJ*, 770, L24
 Kramer, M. & Champion, D. J. 2013, *Classical and Quantum Gravity*, 30, 224009
 Lazio, T. J. W. & Cordes, J. M. 1998, *ApJ*, 505, 715
 Liu, K., Wex, N., Kramer, M., Cordes, J. M., & Lazio, T. J. W. 2012, *ApJ*, 747, 1
 Macquart, J.-P., Kanekar, N., Frail, D. A., & Ransom, S. M. 2010, *ApJ*, 715, 939
 Mori, K., Gotthelf, E. V., Zhang, S., et al. 2013, *ApJ*, 770, L23
 Shannon, R. M. & Johnston, S. 2013, *MNRAS*, 435, L29
 Spitler, L. G., Lee, K. J., Eatough, R. P., et al. 2014, *ApJ*, 780, L3
 van Langevelde, H. J., Frail, D. A., Cordes, J. M., & Diamond, P. J. 1992, *ApJ*, 396, 686
 Wucknitz, O. 2013, *PoS(11th EVN Symposium)049*, arXiv:1308.3976